WOOD RESEARCH
63 (1): 2018
105-116

PERFORMANCE EVALUATION OF THE BENDING STRENGTH OF LARCH CROSS-LAMINATED TIMBER

Yo-Jin Song, Soon-Il Hong
Kangwon National University, College of Forest and Environmental Sciences
Division of Forest Material Science
and Engineering
Chuncheon, Republic of Korea

(Received January 2017)

ABSTRACT

A bending strength test was carried out on the strip-type cross-laminated timber (3 layers) that was combined differently by the cross-sectional annual ring orientation of the laminae under the same modulus of elasticity combination. In addition, the bending modulus of elasticity and the maximum bending moment predicted using the gamma method were compared with the results of the actual test.

The result of the bending strength test showed no significant difference in bending strength among the specimens combined according to the annual ring orientation. Furthermore, when the outer tension layer of the cross-laminated timber was strengthened with a glass-fiber-reinforced plastic plate (volume ratio: 1.2%), the modulus of elasticity and the modulus of rupture increased by 4.2% and 16.3%, respectively. The ratios of the prediction results for the bending modulus of elasticity and the maximum bending moment by the gamma method to the actual test values were 1.01 and 0.96 on average, respectively, indicating that the two values were almost identical.

KEYWORDS: *Larix kaempferi* Carr., cross-laminated timber, bending strength, gamma method, glass fiber reinforcement.

INTRODUCTION

Cross-laminated timber (CLT) is a structural wood panel made of laminae with thicknesses of around 20-60 mm, which are laminated orthogonally to the fiber direction to resist in the positive direction of the load (Schmidt and Griffin 2009). CLT is gaining popularity of late in Europe as interior and exterior members because it is versatile and suitable for high-rise buildings (Van de Kuilen 2010, Gagnon and Pirvu 2011). Unlike glulam with a column-beam structure, the CLT construction method is a panel-panel structure, in which the CLT itself becomes the wall, flooring, and roof. Thus, strength against the vertical and horizontal loads of the CLT panel

itself is required. The CLT wall requires compressive and buckling strength against the vertical load, bending and shear strength against the wind load, and shear and joint strength against earthquakes. For the CLT flooring and roof, the load capacity for bending shear, and compressive due to the short- and long-term vertical loads should be considered (Japan CLT Association, 2013). Among them, the bending load capacity against the short-term load is one of the factors that must be evaluated first when using CLT for the wall and flooring. As such, many studies have been conducted on the bending strength of CLT. Sikora et al. (2016) researched on the correlation between the bending strength and the rolling shear according to the CLT panel thickness. They reported that the bending stress increased when the panel became thinner, and that the rolling shear strength is adversely affected by an increase in the panel thickness. Steiger et al. (2012) argued that because CLT is used as panel and beam elements, exclusive test standards for CLT were required, as for glulam and solid timber. Wang et al. compared and analyzed the mechanical behaviors of three hybrid CLTs (HCLTs) fabricated using lumber and laminated strand lumber to complement the bending strength performance of the existing CLT. As a result, the modulus of elasticity (MOE) and modulus of rupture (MOR) of HCLT increased by 13-19% and 24-36%, respectively, compared to those of the existing CLT (Wang et al. 2015). Furthermore, Choi et al. (2015) used plywood instead of lumber in the core layer, and reported that the MOR improved by 59.6%, showing a similar bending strength as glulam. Studies comparing the predicted values by designing with the properties obtained through an actual bending strength test were also carried out. Okabe et al. tested the bending strength of CLT according to the MOE, thickness, and number of layers, and predicted the bending stiffness and moment carrying capacity using the Monte Carlo simulation method, based on the test results. They confirmed that the calculated bending stiffness coincided with the result of the actual test. They also reported that the moment carrying capacity calculated using the deterministic design method was underestimated (Okabe et al. 2014). Park et al. evaluated the bending strength of CLT panels produced with six species of trees, including softwood and hardwood. They reported that the MOE and MOR increased as the specific gravity of the trees became higher, and that there was little difference between the values calculated from the individual MOE of the laminae and the MOE values of the CLT panels obtained from the test (Park et al. 2016).

Meanwhile, various problems may occur due to the shrinkage and swelling that occur in each lamina because CLT is cross-laminated, unlike glulam. Thus, in a preliminary study, a delamination strength test was conducted on the CLTs that were combined differently according to the cross-sectional annual ring orientation of the lamina. As a result, the delamination rate of the combination was lowest when the annual ring orientation of the outer lamina was directed inward, and highest when the annual ring orientation of the outer lamina was directed outward (Song and Hong 2016). In this study, therefore, to verify the correlation between the annual ring orientation of the laminae and the bending strength, the bending strength performance was tested by selecting the combinations with the highest and lowest delamination rates in the preliminary study, and the bending strength properties were predicted and compared with the actual test value.

MATERIALS AND METHODS

Testing materials

In this study, domestic larch (*Larix kaempferi* Carr.) laminae with no vertical joint and with a 13% average air-dry moisture content, a 0.52 average air-dry specific gravity, and a 27 (T) × 89 (W) mm size were used. These laminae were graded according to KS F 3021, through longitudinal vibration measurement (KS F 3021, 2013).

Production of specimens for the bending strength test

The bending strength test specimens were made of three layers. The MOE was E13 for the outer tension laminae, E7 to E9 randomly for the middle laminae, and E11 for the outer compression laminae. The specimens were laminated with phenol-resorcinol formaldehyde resin (PRF), the amount of applied resin was set at 400 g·m^{-2} (single spread), and the compression pressure was set at 0.9 N·mm^{-2} (CLT Handbook, 2011).

The bending strength test specimens were fabricated in four types, as shown in Fig. 1. Type A was a combination that showed the lowest delamination rate in the preliminary study (Song and Hong 2016).

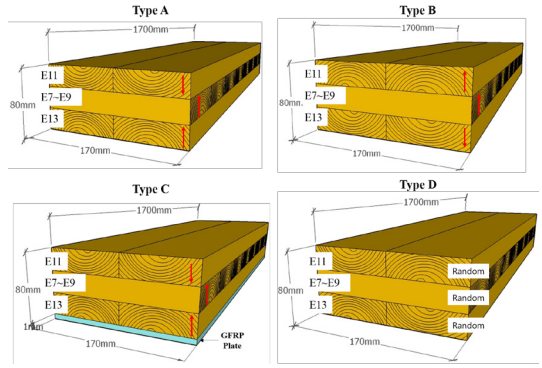

Fig. 1: Bending test specimens combined according to the cross-sectional annual ring orientation of the laminae.

It was composed in such a way that the annual ring orientation on the cross-section of the outer laminae was directed inward, and the annual ring orientation of the middle laminae was directed upward. On the other hand, Type B was a combination that showed the highest delamination rate in the preliminary study. It was composed in such a way that the annual ring orientation on the cross-section of the outer laminae was directed outward, and the annual ring orientation of the middle laminae was directed upward. Type C had the same combination as Type A, but with a glass-fiber-reinforced plate (GFRP) on the surface of the outer tension laminae for reinforcement, at a volume ratio of 1.2%. The GFRP plate was attached to the CLT surface with polyvinyl acetate resin (PVAc) (Park et al. 2009). Type D was a specimen with a random combination of the annual ring orientations of the cross-section, and the MOE combination was identical to those of the previous specimens. The specimens were cured at room temperature for more than 24 hours after compression, and the final size after curing was 81 (T) × 170 (W) × 1700 (L) mm. Seven specimens were fabricated for each type.

Prediction and design of the bending performance of larch CLT

Prediction of the MOE using longitudinal vibrations

Before the bending strength test, a Free-Field Pre-polarized Microphone (Make: G.R.A.S, Type 40AE) was installed on the cross-section of the CLT bending strength test specimens, and the natural frequency of the longitudinal vibration was measured by applying impact to the cross-section on the opposite side. Then the MOE was calculated from the measured natural frequency using the following equation:

$$E_L = \left(\frac{2f_n L}{n}\right)^2 \cdot \rho \quad (1)$$

where: E_L - MOE by the proper vibration of the longitudinal vibration (N·mm^{-2}),
f_n - natural frequency of the n-th degree (Hz),
ρ - density (g·mm^{-3}),
L - length of the specimen (mm).

Design according to the mechanically jointed beams theory (gamma method)

In the CLT Handbook, the design of the bending MOE and the bending moment of the CLT is based on the mechanically jointed beam theory, a method of designing the glulam beam produced by joint metals, and on the composite theory used for plywood design.

The lower the span-to-depth ratio of the CLT is, the more it is affected by the shear deformation of the middle layer. The composite theory should be applied when the span-to-depth ratio is greater than 30 because it does not take into account the rolling shear modulus of the middle layer (Blass 2004). In this study, the bending MOE and the bending moment of CLT were designed based on the mechanically jointed beam theory because the span-to-depth ratio was 18.

According to the CLT Handbook and Mestek, the shear modulus of softwoods is generally 1/16 of the MOE, and the rolling shear modulus is 1/10 of the shear modulus

(CLT Handbook 2011, Mestek et al. 2008). Thus, in Europe, CLT is designed by setting the G_R at 50 MPa, which is smaller than the original G_R, after calculating E=9500 MPa,

G=595 MPa, and G_R=59.5 MPa based on SPF Lumbers No.1/No.2. In this study, the dynamic moduli of elasticity of 320 larch laminae were measured using the natural frequency of the longitudinal vibrations, and the obtained values were substituted into Eq. 3 to calculate the rolling shear modulus.

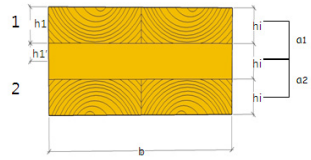

Fig. 2: Cross-section of a three-layer CLT panel.

$$E = \frac{EI_{eff}}{I}, EI_{eff} = \sum(E_i I_i + \gamma_i E_i A_i a_i^2) \quad (2)$$

$$G = \mathrm{E}/16,\ G_r = /10 \quad (3)$$

$$\gamma_i = \frac{1}{1+\pi^2 \frac{E_i A_i h_1'}{l^2 G_r b}} \quad (4)$$

$$\sigma_{max} = \sigma_{global} + \sigma_{local}$$

$$\sigma_{global} = \frac{\gamma_i E_i a_i M}{(EI)_{eff}}$$

$$\sigma_{local} = \frac{0.5 E_i h_i M}{(EI)_{eff}}$$

$$\sigma_{max} = \frac{M E_i}{(EI)_{eff}} \cdot (\gamma_i a_i + 0.5 h_i)$$

$$\sigma_{max} = \sigma_{global} + \sigma_{local} \leq \emptyset \cdot F_b$$

$$M = \emptyset \cdot F_b \cdot \frac{(EI)_{eff}}{E_i(\gamma_i a_i + 0.5h_i)}$$

where: E - MOE by gamma method (MPa),
E_i - MOE of panel (MPa),
I_{eff} - effective moment of inertia,
I - geometrical moment of inertia,
A - cross section (mm^2),
l - span (mm),
h - specimen thickness (mm),
a - distance between the central axis of each panel (mm),
Gr - rolling shear modulus,
γ - connection efficiency factor ($0 < \gamma \leq 1$),
M - bending moment (kN•m),
$\emptyset$ - resistance factor (0.9),
F_b - reference bending strength (MPa).

Bending test method

The bending strength test of the larch CLT was carried out using the 4-point load method (Fig. 3). The span was set to 1500 mm (18h ± 3h), the distance between the loading points to 200 mm, and the test speed to 5 mm·min^{-1} (prEN 16351:2013). To measure the displacement, two displacement transducers (CDP-50) were installed in the front and back at the center of the specimen, and the average value of the deformation of two displacement transducers was used for the analysis of the results. The MOE and MOR were determined by substituting the test results into Eqs. 5 and 6 respectively.

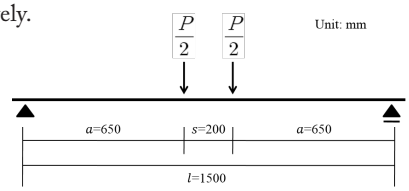

Fig. 3: Schematic diagram of the bending test of CLT.

$$MOE = \frac{\Delta P a(3l^2 - 4a^2)}{48I3\Delta V} \quad (5)$$

$$MOR = \frac{3P_{max}(l-s)}{2b\,h^2} \quad (6)$$

where: P_{max} - maximum load (N),
ΔP - proportional limit load (N),
ΔV - proportional limit deformation (mm,)
l - span (mm),
s - distance between the loading points (mm),
b - specimen width (mm),
h - specimen thickness (mm)
a - distance between the supporting and loading points (mm),
I - geometrical moment of inertia.

RESULTS AND DISCUSSION

Performance evaluation of the bending strength of larch CLT

Load-deformation curve

The average MOE and MOR of Type A, which were the lowest in the preliminary test, were determined to be 9.5 GPa and 47.1 MPa, respectively (Tab. 1). On the other hand, the average MOE and MOR of Type B, which had the highest delamination rate, were determined to be 9.2 GPa and 43.9 MPa, respectively. The MOE of Type B was similar to that of Type A, but the MOR was 7% lower. The average MOE and MOR of Type C, which had the same combination as Type A but had been reinforced with a GFRP outside the outer tension laminae, were determined to be 10.2 GPa and 55.3 MPa, respectively. The average MOE and MOR of Type C were 7 and 17% higher, respectively, than those of Type A. The reinforcement by the GFRP contributed more to the MOR than to the MOE and to the stiffness of the larch CLT. A similar trend was observed in the studies conducted by Park (2009) reported that the MOE and MOR increased by 9 and 12%, respectively, when a larch glulam was reinforced with a GFRP at the volume ratio of 0.7%. Furthermore, Raftery and Harte (2011) reported that when a spruce glulam was reinforced with a GFRP at the volume ratio 1.26%, the MOE and MOR increased by 16 and 38%, respectively. Thus, the MOR increased more than the MOE. The reason that the MOR increased more than the MOE did is that the GFRP suppresses fracture in the tension side and causes compression fracture (Gentry 2011). The average MOE and MOR of the randomly combined Type D were 10.1 GPa and 46.5 MPa, respectively. The average MOE was 6% higher than that of Type A, but the average MOR was similar. The test results confirmed that most of the specimens showed elastic behavior (Fig. 4).

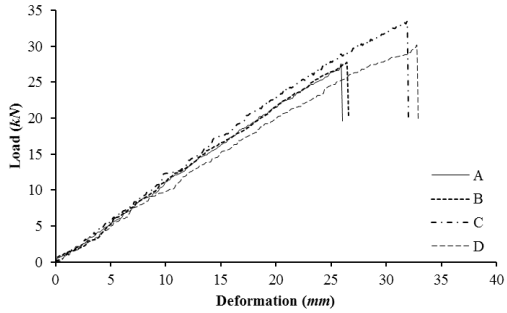

Fig. 4: Typical load-deformation curves of the static bending test.

Tab. 1: Bending test results for the CLT loaded perpendicular to the plane.

Specimen	No.	Density (kg·m3)	MOE (GPa)	Ave. MOE (GPa)	MOR (MPa)	Ave. MOR (MPa)	Stiffness (kN·mm1)	Ave. Stiffness (kN·mm1)	Failure mode
Type A	1	520	9.3	9.5	39.8	47.1	1.0	1.0	Delamination
	2	538	9.2		42.4		1.0		Delamination
	3	575	11.4		59.0		1.2		Tensile
	4	565	10.3		49.1		1.1		Tensile
	5	559	9.7		48.0		1.0		Delamination
	6	504	8.4		49.2		0.9		Delamination
	7	516	8.5		42.2		0.9		Tensile
Type B	1	517	9.1	9.2	41.1	43.9	1.0	1.0	Tensile
	2	520	10.5		49.7		1.1		Tensile
	3	487	7.5		32.2		0.8		Tensile
	4	483	7.7		34.0		0.8		Tensile
	5	544	9.8		57.6		1.1		Tensile
	6	528	10.5		50.4		1.1		Tensile
	7	527	9.1		42.5		0.9		Tensile
Type C	1	534	10.2	10.2	52.4	55.3	1.1	1.2	Delamination
	2	575	10.2		35.8		1.1		Delamination
	3	579	11.1		56.9		1.2		Tensile
	4	574	9.9		73.6		1.1		Delamination
	5	567	10.6		58.5		1.2		Delamination
	6	528	9.8		49.4		1.2		Delamination
	7	554	9.6		59.0		1.2		Delamination
Type D	1	524	10.7	10.1	43.3	46.5	1.1	1.1	Tensile
	2	519	9.5		48.7		1.0		Tensile
	3	528	8.9		54.0		0.9		Delamination
	4	547	9.9		35.7		1.1		Tensile
	5	535	11.5		36.9		1.2		Tensile
	6	533	10.0		55.7		1.1		Tensile
	7	546	10.5		51.4		1.1		Tensile

Failure mode

As a result of the bending strength test, two failure modes occurred, as shown in Fig. 5. Tension failure is the case where the outer tension laminae start to fracture first at the center of the specimen when the maximum load is applied, and then the fracture progresses to the compression side along the middle lamina. This failure mode occurred when the outer laminae were quarter- or rift- swan, when there were knots or other defects in the center of the outer tension laminae, when the annual ring orientations of the outer tension laminae were all directed outward, and when they were mixed. Tension failure occurred in 60% of all the specimens and was mostly observed in Type B, where the cross-sectional annual ring orientations of all the outer tension laminae were directed outward, and in Type D, which was a random combination.

Delamination failure is the case where the outer tension laminae are not fractured at the maximum load, and a rolling shear is generated in the middle layer, resulting in a complete fracture along the glue-line all the way to the end of the cross-section.

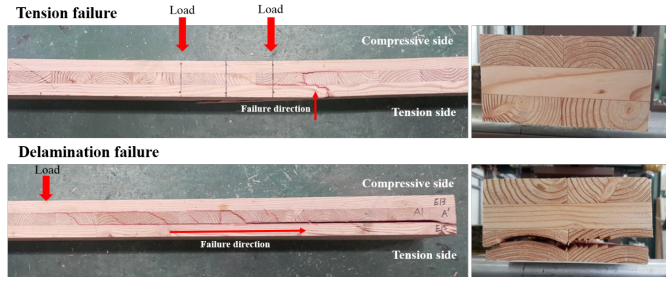

Fig. 5: Failure modes of the static bending test of the CLT.

This failure mode occurred when there were no defects (e.g., a knot) in the center of the outer tension laminae, and when the annual ring orientations on the cross-section of the outer tension laminae were directed inward. This tendency was the same as that of the delamination test failure mode according to the cross-sectional annual ring orientation in the preceding study (Song and Hong 2016). Delamination failure occurred in 40% of all the specimens and was mainly observed in Type A, where all the cross-sectional annual ring orientations of the outer tension laminae were directed inward, and in Type C, which was reinforced with the same combination. In particular, the fractures of Type A occurred in the glue-line of the tension side whereas Type C failed in the glue-line of the compression side, thus positively confirming the reinforcing effect. Such reinforcing effect can be greater if the outer tension laminae are defective or low-grade, with a low MOE (Raftery and Harte 2011).

Meanwhile, in the study conducted by Sikora et al. (2016) the specimens where delamination failure occurred had low strength, which was attributed to the lack of quality control in the bonding process. In this study, however, the average MOR of tension failure was 45.6 ± 8.4 MPa, and the average MOR of delamination failure was 46.7 ± 5.6 MPa. Thus, there was no difference in strength between tension failure and delamination failure, unlike in the study conducted by Sikora et al. (2016). The annual ring orientation of the laminae in the tension side appeared to have the greatest effect on the failure mode.

Prediction and design of the bending performance of larch CLT

The average rolling shear modulus of 320 larch laminae for the gamma method design was 72 MPa, and the assumed value (70 MPa) was substituted into Gr. The γ (connection efficiency factor) value determined using this ranged from 0.75 to 0.81. For the reference bending strength (Fb) value that was used in the design of the maximum bending moment through the gamma method, 50 MPa was applied, which was estimated from the 5% lower exclusion limit for the larch bending strength test results obtained by Hwang et al. (2011).

As a result of the MOE analysis, the E_{Lv} obtained through the longitudinal vibration method was slightly lower than the E_b (E_{Lv}/E_b=0.89). In the case of Type C, it was unclear if the GFRP plate influenced the natural frequency of the longitudinal vibration. In the case of Type C, the design value was determined to be lower than the measured value because the information on the GFRP plate was not included in the design process during the prediction design using the gamma method. Therefore, the E_{Gm}/E_b values of Type A, B, and D (excluding that of Type C) were 1.02, indicating that the measured and design values are almost identical. As a result of the analysis of the maximum bending moment, the M_{Gm}/M_b ratios of all the specimens except Type C were almost identical (0.98) (Tab. 2).

Tab. 2: Comparison of the properties determined through the static bending test and the properties determined through the design method.

Specimen		E_b	E_{Lv}	E_{Gm}	M_b	M_{Gm}	E_{Lv}/E_b	E_{Gm}/E_b	M_{Gm}/M_b
	Unit	*MPa*			*kN•m*				
Type A	1	9.3	9.3	10.2	7.21	7.66	1.00	1.10	1.06
	2	9.2	9.5	10.2	7.69	7.66	1.03	1.11	1.00
	3	11.4	9.4	10.5	10.77	7.65	0.82	0.92	0.71
	4	10.3	9.5	10.5	8.95	7.65	0.92	1.02	0.86
	5	9.7	8.7	9.4	8.63	7.70	0.90	0.97	0.89
	6	8.4	7.6	9.4	8.97	7.78	0.90	1.11	0.87
	7	8.5	7.5	9.1	7.64	8.00	0.88	1.08	1.05
Average		9.5	8.8	9.9	8.6	7.7	0.9	1.0	0.9
SD		1.0	0.8	0.5	1.1	0.1	0.1	0.1	0.1
Type B	1	9.1	9.1	9.9	7.45	7.68	1.00	1.09	1.03
	2	10.5	8.8	9.9	9.01	7.68	0.84	0.94	0.85
	3	7.5	7.0	8.7	5.81	7.74	0.93	1.16	1.33
	4	7.7	7.3	8.7	6.13	7.74	0.95	1.13	1.26
	5	9.8	8.7	10.1	10.56	7.67	0.89	1.03	0.73
	6	10.5	8.9	9.7	9.19	8.00	0.84	0.92	0.87
	7	9.1	7.8	9.1	7.80	8.64	0.85	1.00	1.11
Average		9.2	8.2	9.4	8.0	7.9	0.9	1.0	1.0
SD		1.1	0.8	0.6	1.6	0.3	0.1	0.1	0.2
Type C	1	10.2	8.8	9.2	9.91	7.69	0.86	0.90	0.78
	2	10.2	9.2	9.4	6.70	7.69	0.90	0.92	1.15
	3	11.1	9.3	9.4	10.67	7.69	0.84	0.85	0.72
	4	9.9	9.1	9.4	13.81	7.69	0.92	0.95	0.56
	5	10.6	9.8	9.4	10.86	7.69	0.92	0.89	0.71
	6	9.8	8.1	9.2	9.71	7.87	0.83	0.94	0.81
	7	9.6	8.8	9.2	11.76	7.92	0.92	0.95	0.67
Average		10.2	9.0	9.3	10.5	7.7	0.9	0.9	0.8
SD		0.5	0.5	0.1	2.0	0.1	0.0	0.0	0.2
Type D	1	10.7	8.6	10.0	7.85	7.68	0.80	0.93	0.98
	2	9.5	8.0	9.6	8.82	7.69	0.84	1.01	0.87
	3	8.9	8.2	9.6	9.79	7.69	0.92	1.08	0.79
	4	9.9	8.7	9.7	6.51	7.69	0.88	0.98	1.18
	5	11.5	8.4	9.7	6.74	7.69	0.73	0.84	1.14
	6	10.0	8.3	9.5	10.22	7.92	0.83	0.95	0.77
	7	10.5	8.7	9.5	9.43	7.93	0.83	0.90	0.84
Average		10.1	8.4	9.7	8.5	7.8	0.8	1.0	0.9
SD		0.8	0.2	0.2	1.4	0.1	0.1	0.1	0.2

Eb: Bending MOE determined through the static bending test; E_{Lv}: MOE determined through the longitudinal vibration method; E_{Gm}: MOE determined through the gamma method; M_b: Maximum bending moment determined through the static bending test; M_{Gm}: Maximum bending moment determined through the gamma method; SD: Standard deviation.

CONCLUSIONS

To improve the quality of the CLT panel, bending strength tests of different combinations of CLT were conducted according to the cross-sectional annual ring orientation of the laminae, and the bending properties predicted by the design were compared with the actual test results. As a result, the design values obtained using the gamma method coincided with the actual test values. Furthermore, the fracture modes were clearly distinguished, although the difference in the bending performance was small according to the combination based on the annual ring orientation. In particular, the sawing direction of the laminae used for the tension side had a great effect on the failure mode. There was no difference in strength, however, between tension failure and delamination failure. The results of this study and the results of the delamination strength test performed in the previous study suggest that if the cross-sectional annual ring orientation of the outer laminae is directed inward during the production of CLTs, both the delamination strength and the bending strength can be satisfactory.

REFERENCES

1. Choi, C., Yuk, C.R., Yoo, J.C., Park, J.Y., Lee, C.G., Kang, S.G., 2015: Physical and mechanical properties of cross laminated timber using plywood as core layer, Journal of The Korean Wood Science and Technology 43(1): 86~95.
2. EN 408, 2012: Timber structures-Structural timber and glued laminated timber-Determination of some physical and mechanical properties.
3. Fellmoser, P., Blass, H.J., 2004: Influence of rolling shear modulus on strength and stiffness of structural bonded timber elements. CIB-W18 (37- 6- 5).
4. Gagnon, S., Pirvu, C., 2011: CLT Handbook: Cross-Laminated Timber. Vancouver, British Columbia: FPInnovations.
5. Gentry, T.R., 2011: Performance of glued-laminated timbers with FRP shear and flexural reinforcement, ASCE Journal of Composites for Construction 15(5): 861-870.
6. Hwang, K.H., Park, J.S., Park, M.J., 2011: Structural performance evaluation by grade for domestic softwood.
7. KSF 3021, 2013: Structural glued laminated timber.
8. Mestek, P., Kreuzinger, H., Winter, S., 2008: Design of cross laminated timber (CLT). Proceedings of the 10th World Conference in Timber Engineering, Miyazaki, Japan.
9. Okabe, M., Yasumura, M., Kobayashi, K., Fujita, K., 2014: Prediction of bending stiffness and moment carrying capacity of sugi cross-laminated timber, The Japan Wood Research Society 60:49-58.
10. Park, H.M., Fushitani, M., Byeon, H.S., Yang, J.K., 2016: Static bending strength performances of Cross-laminated wood panels made with six species, Wood and Fiber Science 48(2): 1-13.
11. Park, J.C., 2009: Strength properties of hybrid fiber-reinforced-plastic reinforced glulam beams. Department of Wood Science and Engineering Graduate School, Kangwon National University.
12. Park, J.C., Shin, Y.J., Hong, S.I., 2009: Bonding performance of glulam reinforced with glass fiber- reinforced plastics, Journal of the Korean Wood Science and Technology 37(4): 357-363.

13. Raftery, G.M., Harte, A. M., 2011: Low-grade glued laminated timber reinforced with FRP plate. Composites: Part B 42(4):724-735.
14. Schmidt, J., Griffin, C.T., 2009: Barriers to the design and use of cross-laminated timber structures in high-rise multi-family housing in the United States. Portland: Department of Architecture, Portland State University.
15. Sikora, K.S., McPolin, D.O., Harte, A.M., 2016: Effects of the thickness of cross-laminated timber (CLT) panels made from Irish Sitka spruce on mechanical performance in bending and shear, Construction and Building Materials 116:141-150.
16. Song, Y.J., Hong, S.I., 2016: Evaluation of bonding strength of larch cross-laminated timber, Journal of the Korean Wood Science and Technology 44(4): 607-615.
17. Steiger, R., Gülzow, A., Czaderski, C., Howald, T., Niemz, P., 2012: Comparison of bending stiffness of cross-laminated solid timber derived by modal analysis of full panels and by bending tests of strip-shaped specimens, Eur. J. Wood Prod. 70:141-153.
18. Van de Kuilen, J. W., Ceccotti, A., Xia, Z., He, M., Li, S., 2010: Wood Concrete Skyscraper. In: Proceeding of the 11th World Conference on Timber Engineering, Trentino, Italy, 492-501.
19. Wang, Z., Gong, M., Chui, Y.H., 2015: Mechanical properties of laminated strand lumber and hybrid cross laminated timber, Construction and Building Materials 101: 622-627.

Yo-Jin Song, Soon-Il Hong*
Kangwon National University
College of Forest and Environmental Sciences
Division of Forest Material Science and Engineering
Chuncheon 24341
Republic of Korea
Phone: +82 33 250 8328
Corresponding author: hongsi@kangwon.ac.kr